



Attenuation of Rheumatoid Inflammation by Sodium Butyrate Through Reciprocal Targeting of HDAC2 in Osteoclasts and HDAC8 in T Cells

Da Som Kim¹, Jeong-Eun Kwon¹, Seung Hoon Lee^{1,2}, Eun Kyung Kim¹, Jun-Geol Ryu¹, Kyung-Ah Jung³, Jeong-Won Choi¹, Min-Jung Park¹, Young-Mee Moon¹, Sung-Hwan Park⁴, Mi-La Cho^{1,5,6*} and Seung-Ki Kwok^{4*}

OPEN ACCESS

Edited by:

Rolando Cimaz,
Università degli Studi di Firenze,
Italy

Reviewed by:

Jason Weinstein,
Yale University, United States
Theresa T. Lu,
Weill Cornell Medicine,
Cornell University, United States

*Correspondence:

Mi-La Cho
iammila@catholic.ac.kr;
Seung-Ki Kwok
seungki73@catholic.ac.kr

[†]These authors have contributed
equally to this work.

Specialty section:

This article was submitted
to Autoimmune and
Autoinflammatory Disorders,
a section of the journal
Frontiers in Immunology

Received: 15 February 2018

Accepted: 20 June 2018

Published: 06 July 2018

Citation:

Kim DS, Kwon J-E, Lee SH, Kim EK,
Ryu J-G, Jung K-A, Choi J-W,
Park M-J, Moon Y-M, Park S-H,
Cho M-L and Kwok S-K (2018)
Attenuation of Rheumatoid
Inflammation by Sodium Butyrate
Through Reciprocal Targeting
of HDAC2 in Osteoclasts
and HDAC8 in T Cells.
Front. Immunol. 9:1525.
doi: 10.3389/fimmu.2018.01525

¹The Rheumatism Research Center, College of Medicine, Catholic Research Institute of Medical Science, The Catholic University of Korea, Seoul, South Korea, ²Division of Immunology, Department of Microbiology and Immunobiology, Harvard Medical School, Boston, MA, United States, ³Impact Biotech, Seoul, South Korea, ⁴Division of Rheumatology, Department of Internal Medicine, Seoul St. Mary's Hospital, College of Medicine, The Catholic University of Korea, Seoul, South Korea, ⁵Laboratory of Immune Network, Conversant Research Consortium in Immunologic Disease, College of Medicine, The Catholic University of Korea, Seoul, South Korea, ⁶College of Medicine, The Institute for Aging and Metabolic Diseases, The Catholic University of Korea, Seoul, South Korea

Rheumatoid arthritis (RA) is a systemic autoimmune disease caused by both genetic and environmental factors. Recently, investigators have focused on the gut microbiota, which is thought to be an environmental factor that affects the development of RA. Metabolites secreted by the gut microbiota maintain homeostasis in the gut through various mechanisms [e.g., butyrate, which is one of the major metabolites of gut microbiota, exerts an anti-inflammatory effect by activating G-protein-coupled receptors and inhibiting histone deacetylases (HDACs)]. Here, we focused on the inhibition of the HDACs by butyrate in RA. To this end, we evaluated the therapeutic effects of butyrate in an animal model of autoimmune arthritis. The arthritis score and incidence were lower in the butyrate-treated group compared to the control group. Also, butyrate inhibited HDAC2 in osteoclasts and HDAC8 in T cells, leading to the acetylation of glucocorticoid receptors and estrogen-related receptors α , respectively. Additionally, control of the T_H17/T_{reg} cell balance and inhibition of osteoclastogenesis were confirmed by the changes in target gene expression. Interleukin-10 (IL-10) produced by butyrate-induced expanded T_{reg} cells was critical, as treatment with butyrate did not affect inflammatory arthritis in IL-10-knockout mice. This immune-cell regulation of butyrate was also detected in humans. These findings suggest that butyrate is a candidate agent for the treatment of RA.

Keywords: sodium butyrate, rheumatoid arthritis, histone deacetylases, glucocorticoid receptor, $ERR\alpha$

INTRODUCTION

Rheumatoid arthritis (RA) is an autoimmune disease of unknown etiology that involves joint destruction (1). An intestinal imbalance is involved in RA development, and gut bacteria have various effects on RA (2, 3). Because the gut microbiota plays an important role in maintaining homeostasis, any imbalance can lead to the development of various diseases and systemic effects. In addition to

protecting the intestinal surface from pathogens, it also participates in digestion and affects bone density and immune system development (4). Indeed, the gut microbiota is also involved in bone metabolism (5) and secreted metabolites modulate the T_H17/T_{reg} cell balance (6). For example, segmented filamentous bacteria secrete serum amyloid A, which induces differentiation of T_H17 cells (7, 8). Several bacterial species secrete short-chain fatty acids (SCFAs) (9, 10) (e.g., acetate, butyrate, and propionate), which induce differentiation of T_{reg} cells from naïve $CD4^+$ T cells (9, 11). SCFAs have immunomodulatory activity. For instance, butyrate exerts an anti-inflammatory effect by downregulating IL-12 and upregulating IL-10 (12). Therefore, butyrate may have a therapeutic effect in immune-mediated inflammatory diseases. Indeed, butyrate reportedly has therapeutic efficacy in various animal models of inflammatory diseases [e.g., dextran sodium sulfate-induced colitis, obesity, and graft-versus-host disease (GvHD)] (13–16). Regarding GvHD, allogeneic bone marrow transplant-recipient mice (C57BL/6J \rightarrow BALB/c) exhibited significantly reduced butyrate levels in intestinal tissue. Butyrate treatment strengthened the intestinal epithelial barrier, indicating that butyrate has immunomodulatory activity. Butyrate also inhibits histone deacetylase (HDAC). In inflammatory arthritis, although the abundance of *Faecalibacterium prausnitzii*, a butyrate-producing bacterium, is reduced in enthesitis-related arthritis (17), the direct therapeutic effect of butyrate on RA is unclear. Therefore, both the therapeutic effect of butyrate in RA and the mechanism underlying this effect should be investigated. Here, we assessed the therapeutic effect of butyrate in an animal model of RA. To identify the mechanism underlying its anti-arthritic effect, we also examined the effect of butyrate on effector T-cell differentiation and osteoclastogenesis. Finally, we verified the mechanism of the effect of butyrate.

MATERIALS AND METHODS

Animals

DBA/1J mice, C57BL/6 mice, and IL-10-knockout (KO) (Orient) mice were maintained in groups of five in polycarbonate cages in a specific-pathogen-free environment. They were provided with access to standard mouse chow (Ralston Purina, Gray Summit, MO, USA) and water *ad libitum*. All experimental procedures were approved by the Animal Research Ethics Committee at the Catholic University of Korea (approval numbers, 2017-0070-02 and 2018-0014-01).

Induction of Collagen-Induced Arthritis (CIA) and Treatment With Butyrate

Collagen-induced arthritis was generated in male DBA/1J mice or IL-10-KO mice. Mice were immunized with 100 μ g of chicken type II collagen (CII) (Chondrex Inc., Redmond, WA, USA) dissolved overnight in 0.1 N acetic acid (4 mg/mL) in complete Freund's adjuvant (CFA). The immunizations were performed intradermally into the base of the tail. Two weeks after primary immunization, mice were boosted with 100 μ g of CII in incomplete Freund's adjuvant (Chondrex Inc.). CIA mice were treated with 100 mg/kg sodium butyrate in saline or with saline alone

via intraperitoneal injections three times per week beginning on day 17 after primary immunization. Butyrate was administered during the entire study period.

Clinical Scoring of Arthritis

Mice were considered to have arthritis when significant changes in redness and/or swelling were noted in the digits or in other parts of the paws. Knee-joint inflammation was scored visually after dissection on a scale from 0 to 4 (0, uninfamed; 1, minimal; 2, mild; 3, moderate; and 4, severe inflammation). Scoring was performed by two independent observers.

Histological Analysis

Histological analysis was performed to determine the extent of joint damage. Mice joint tissues were fixed in 4% paraformaldehyde, decalcified in 10% ethylenediaminetetraacetic acid solution, embedded in paraffin, and sectioned. The sections were deparaffinized using xylene and dehydrated through an alcohol gradient. Endogenous peroxidase activity was quenched with methanol–3% H_2O_2 . Sections were staining using hematoxylin and eosin (H&E), safranin O, or tartrate-resistant acid phosphatase (TRAP).

Confocal Microscopy

Naïve $CD4^+$ T cells were placed in the appropriate well of a cyto-spin chamber (Thermo Fisher Scientific, MI, USA) and centrifuged at 700 \times g for 3 min. Tissue cryosections (7- μ m thick) or naïve $CD4^+$ T cells cultured under T_H17 differentiation conditions were fixed with methanol–acetone and stained with fluorescein isothiocyanate (FITC)-, PE-, PerCP-Cy5.5-, or allophycocyanin (APC)-conjugated monoclonal antibodies against mouse CD4, CD25, IL-17, Foxp3, IL-10, DAPI, CPTIA, and NR1D1 (eBioscience, San Diego, CA, USA). After an overnight incubation at 4°C, the stained sections were visualized by confocal microscopy (LSM 510 Meta; Zeiss).

Immunohistochemistry

Immunohistochemistry was performed using the Vectastain ABC kit (Vector Laboratories, Burlingame, CA, USA). Tissue sections were incubated overnight at 4°C with primary antibodies against IL-1 β , IL-6, IL-17, TNF- α , CD68, and secretory leukocyte protease inhibitor (SLPI); probed with a biotinylated secondary antibody; and stained with a streptavidin-peroxidase complex for 1 h. DAB chromogen (Dako, Carpinteria, CA, USA) was added as a substrate, and the samples were visualized by microscopy (Olympus, Center Valley, PA, USA).

Quantification of CII-Specific Antibodies

Blood was obtained from the orbital sinus of CIA mice, and the serum was stored at –20°C until used. The serum levels of antibodies to CII-specific mouse IgG, IgG1, IgG2a, and IgG3 were measured using enzyme-linked immunosorbent assay kits (Bethyl Laboratories, Montgomery, TX, USA).

Mouse *In Vitro* Osteoclastogenesis

Bone marrow-derived monocyte/macrophages (BMMs) were isolated from the tibias and femurs of CIA mice by flushing the bone-marrow cavity with minimum essential medium- α

(Invitrogen, Carlsbad, CA, USA). The cells were incubated for 6 h to separate nonadherent and adherent cells. Non-adherent cells were seeded in 48-well plates at 2×10^5 cells/well and cultured in the presence of 10 ng/mL rh M-CSF (R&D Systems, Minneapolis, MN, USA) for 3 days to form macrophage-like osteoclast precursor cells (preosteoclasts). Three days later, the nonadherent cells were washed out, and preosteoclasts were cultured in the presence of 10 ng/mL M-CSF, 50 ng/mL RANKL (Peprotech, London, UK), and various concentrations of sodium butyrate for 4 days to generate osteoclasts. On day 2, the medium was replaced with fresh medium containing M-CSF, RANKL, and sodium butyrate.

For osteoclast staining for SLPI, BMM of CIA-induced mice were separated into non-adherent and adherent cells, and the former were cultured with M-CSF on 8-well cell culture slides for 3 days. After 3 days, preosteoclasts were removed and cultured in the presence of M-CSF and RANKL. After 1 day, medium was washed and incubated for 1 day in the presence of 100 μ M and 1 mM sodium butyrate.

Mouse *Ex Vivo* Osteoclastogenesis

Bone marrow-derived monocyte/macrophages were isolated from the tibias and femurs of IL-10-KO mice 11 weeks after CIA induction. These cells were seeded under the same conditions used for mouse *in vitro* osteoclastogenesis; after 3 days, they were stimulated with the same concentrations of M-CSF and RANKL. Preosteoclasts were cultured for 3 days to generate osteoclasts; on day 2, the medium was replaced with fresh medium containing M-CSF and RANKL.

Human *In Vitro* Osteoclastogenesis

Peripheral blood mononuclear cells (PBMCs) obtained from normal healthy humans were separated from buffy coats using Ficoll-Hypaque (Pharmacia Biotech, Piscataway, NJ, USA). Red blood cells were removed, and the cells were seeded into 24-well plates at 5×10^5 cells/well and incubated at 37°C for 2 h to separate non-adherent and adherent cells. The adherent cells were washed with phosphate-buffered saline and cultured with 100 ng/mL M-CSF for 3 days. After 3 days, these preosteoclasts were cultured in the presence of 25 ng/mL M-CSF, 30 ng/mL RANKL, and various concentrations of sodium butyrate for 6 days to generate osteoclasts. On day 3, the medium was replaced with fresh medium containing M-CSF, RANKL, and sodium butyrate. All human experimental procedures were approved by the Ethics Committee of Seoul St. Mary's Hospital (Seoul, Republic of Korea, KC17TNSI0570) and written informed consent was obtained.

TRAP Staining

A commercial TRAP staining kit (Sigma-Aldrich, St. Louis, MO, USA) was used according to the manufacturer's instructions. TRAP-positive multinucleated cells (MNCs) containing at least three nuclei were counted as osteoclasts.

Real-Time Polymerase Chain Reaction (PCR)

Messenger RNA (mRNA) was extracted using TRI Reagent (Molecular Research Center, Inc., Cincinnati, OH, USA) according

to the manufacturer's instructions. Complementary DNA was synthesized using a Super Script Reverse Transcription system (TaKaRa, Shiga, Japan). A Light-Cycler 2.0 instrument (software version 4.0; Roche Diagnostics) was used for PCR amplification. All reactions were performed using the LightCycler FastStart DNA Master SYBR Green I mix (TaKaRa) following the manufacturer's instructions. The following primers were used: Carbonic anhydrase II, 5'-TGG-TTC-ACT-GGA-ACA-CCA-AA-3' (sense) and 5'-AGC-AAG-GGT-CGA-AGT-TAG-CA-3' (antisense); TRAP, 5'-TCC-TGG-CTC-AAA-AAG-CAG-TT-3' (sense) and 5'-ACA-TAG-CCC-ACA-CCG-TTC-TC-3' (antisense); integrin β 3, 5'-CCA-CAC-GAG-GCG-TGA-ACT-3' (sense) and 5'-CTT-CAG-GTT-ACA-TCG-GGG-TGA-3' (antisense); DC-stamp, 5'-GCA-CGC-AAT-CGC-GTC-AAC-T-3' (sense) and 5'-AGG-CAT-TCC-GTC-TGC-TTT-GA-3' (antisense); matrix metalloproteinase-9 (MMP-9), 5'-CTG-TCC-AGA-CCA-AGG-GTA-CAG-CCT-3' (sense) and 5'-GAG-GTA-TAG-TGG-GAC-ACA-TAG-TGG-3' (antisense); calcitonin receptor, 5'-CGG-ACT-TTG-ACA-CAG-CAG-AA-3' (sense) and 5'-AGC-AGC-AAT-CGA-CAA-GGA-GT-3' (antisense); HDAC1, 5'-CTA-TGC-TGT-GAA-CTA-CCC-ACT-G-3' (sense) and 5'-GGA-ATC-TGA-GCC-ACA-CTG-TAA-G-3' (antisense); HDAC2, 5'-CAT-GGC-GTA-CAG-TCA-AGG-AG-3' (sense) and 5'-AGC-AAG-TTA-TGA-GTC-ATC-CGG-3' (antisense); HDAC3, 5'-TGT-CTC-AAT-GTG-CCC-TTA-CG-3' (sense) and 5'-CCT-AAT-CGA-TCA-CAG-CCC-AG-3' (antisense); HDAC4, 5'-AGC-ACT-GAG-AAT-GGC-ATC-G-3' (sense) and 5'-TGA-TGT-TGG-GTA-AGG-ATG-GTG-3' (antisense); HDAC5, 5'-TTC-AAC-TCC-GTA-GCC-ATC-AC-3' (sense) and 5'-GGA-TCG-TTG-TAG-AAT-GCT-TGC-3' (antisense); HDAC6, 5'-TGC-CCA-CCT-AAC-CCA-TTT-G-3' (sense) and 5'-AAG-CAC-TGA-TTC-CCT-TAG-CC-3' (antisense); HDAC7, 5'-TCA-AAC-TGG-ATA-ACG-GGA-AGC-3' (sense) and 5'-CCA-GAT-GGT-GTC-AGT-ATC-GAC-3' (antisense); HDAC8, 5'-ACC-GAA-TCC-AGC-AAA-TCC-TC-3' (sense) and 5'-CAG-TCA-CAA-ATT-CCA-CAA-ACC-G-3' (antisense); HDAC9, 5'-AGG-ATG-ATG-ATG-CCT-GTG-GTG-GAT-3' (sense) and 5'-GAG-TTG-TGC-TTG-ATG-CTG-CCT-TGT-3' (antisense); HDAC10, 5'-CTG-TCA-ATT-TGC-CCT-GGA-AC-3' (sense) and 5'-CCC-CGA-TAG-CAG-AGT-CAA-ATC-3' (antisense); HDAC11, 5'-GCT-GGG-AAA-TGG-GGC-AAG-GTG-A-3' (sense) and 5'-AGC-TCG-TTG-AGA-TAG-CGC-CTC-GT-3' (antisense); TNF- α , 5'-AAG-CCT-GTA-GCC-CAC-GTC-GTA-3' (sense) and 5'-GGC-ACC-ACT-AGT-TGG-TTG-TCT-TTG-3' (antisense); Foxp3, 5'-GGC-CCT-TCT-CCA-GGA-CAG-A-3' (sense) and 5'-GCT-GAT-CAT-GGC-TGG-GTT-GT-3' (antisense); CTLA4, 5'-TGA-CCC-AAC-CCT-CAG-TGG-TG-3' (sense) and 5'-TTT-GGT-CAT-TTG-TCT-GCC-GC-3' (antisense); CPTIA, 5'-GAT-CTA-CAA-TTC-CCC-TCT-GCT-C-3' (sense) and 5'-AGC-CAG-ACC-TTG-AAG-TAA-CG-3' (antisense); NR1D1, 5'-GCC-ATG-TTT-GAC-TTC-AGC-G-3' (sense) and 5'-AAT-TCT-CCA-TTC-CCG-AGC-G-3' (antisense); SLPI, 5'-GGC-CCT-TTA-CCT-TTC-ACG-GTG-3' (sense) and 5'-GGC-TCC-GAT-TTT-GAT-AGC-ATC-AT-3' (antisense); IL-10, 5'-GGC-CCA-GAA-ATC-AAG-GAG-CA-3' (sense) and 5'-AGA-AAT-CGA-TGA-CAG-CGC-CT-3' (antisense); and β -actin, 5'-GAA-ATC-GTG-CGT-GAC-ATC-AAA-G-3' (sense), and 5'-TGT-AGT-TTC-ATG-GAT-

GCC-ACA-G-3' (antisense). All mRNA levels were normalized to that of β -actin.

Murine T-Cell Isolation and Differentiation

To purify splenic CD4⁺ T cells, splenocytes were incubated with CD4-coated magnetic beads and isolated using magnetic-activated cell sorting (MACS) separation columns (Miltenyi Biotec, Bergisch Gladbach, Germany). MACS-sorted CD4⁺ T cells were sorted to obtain naïve CD4⁺ T cells by selecting for CD4⁺CD62L^{high}CD44^{low}. To establish T_H17 cell-polarizing conditions, the cells were stimulated with anti-CD3 (0.5 μ g/mL), anti-CD28 (1 μ g/mL), anti-interferon- γ (anti-IFN- γ) (1 μ g/mL), anti-IL-4 (2 μ g/mL), IL-6 (40 ng/mL), and transforming growth factor- β (TGF- β) (2 ng/mL) for 3 days. Recombinant mouse IL-6 and antibodies to IFN- γ and IL-4 were purchased from R&D Systems, and TGF- β was purchased from PeproTech.

Human CD4⁺ T-Cell Isolation and Differentiation

CD4⁺ T cells were isolated from human PBMCs using a CD4⁺ T-cell isolation kit (Miltenyi Biotec) according to the manufacturer's instructions. Th0 cells were stimulated with anti-CD3 (0.5 μ g/mL) and anti-CD28 (1 μ g/mL) with no added cytokines. To establish T_H17 cell-polarizing conditions, the CD4⁺ T cells were stimulated with anti-CD3, anti-CD28, anti-IFN- γ (2 μ g/mL), anti-IL-4 (2 μ g/mL), IL-1 β (20 ng/mL), and IL-6 (20 ng/mL) for 3 days. Recombinant human IL-1 β and IL-6 and antibodies to IFN- γ and IL-4 were purchased from R&D Systems, and TGF- β was purchased from Peprotech.

Flow Cytometry

For intracellular staining, cells were restimulated with 25 ng/mL phorbol 12-myristate 13-acetate and 250 ng/mL ionomycin (both from Sigma-Aldrich) for 4 h in the presence of GolgiStop (BD Biosciences, Sparks, MD, USA). Murine splenocytes were stained with surface PerCP-conjugated anti-CD4 (eBioscience) and APC-conjugated anti-CD25 (BioLegend, San Diego, CA, USA) antibodies. After fixation and permeabilization, cells were stained with FITC-conjugated anti-IL-17, APC-conjugated anti-IFN- γ , phycoerythrin (PE)-conjugated anti-IL-4, or PE-conjugated anti-Foxp3 antibodies (eBioscience). Human CD4⁺ T cells were stained with surface PE-Cy7-conjugated anti-CD4 and APC-conjugated anti-CD25 antibodies (BioLegend). After fixation and permeabilization, cells were stained with PE-conjugated anti-IL-17 or PE-conjugated anti-Foxp3 antibodies (eBioscience). Events were collected and analyzed with FlowJo software (Tree Star, Ashland, OR, USA).

Western Blotting

The protein levels of p-STAT3 Y705, p-STAT3 S727, STAT3 (Cell Signaling, Danvers, MA, USA), and GAPDH (Abcam, Cambridge, MA, USA) were measured using a western blot system (SNAP i.d. Protein Detection System, Merck Millipore, Danvers, MD, USA). Total splenocytes or CD4⁺ T cells were preincubated in the presence or absence of sodium butyrate (100, 200, and 500 μ M) for 2 h, cultured with IL-6 (10 ng/mL) for 1 h, and cell lysates were prepared. Protein concentrations were

determined using the Bradford method (Bio-Rad, Hercules, CA, USA), and samples were separated on a sodium dodecyl sulfate polyacrylamide gel and transferred to a nitrocellulose membrane (Amersham Pharmacia, Uppsala, Sweden). The primary antibodies to p-STAT3 Y705, p-STAT3 S727, STAT3, and GAPDH were diluted in 0.1% skim milk in Tris-buffered saline and incubated for 20 min at room temperature. The membrane was washed and incubated with a horseradish peroxidase-conjugated secondary antibody for 20 min at room temperature.

Immunoprecipitation

RAW 264.7 cells were seeded into 100-mm dishes at 1×10^6 cells/dish and cultured overnight with M-CSF (10 ng/mL), RANKL (50 ng/mL), and sodium butyrate (500 μ M). EL4 cells were seeded into 100-mm dishes at 1×10^6 cells and cultured for 2 days in the presence of anti-CD3 (0.5 μ g/mL), IL-6 (10 ng/mL), and sodium butyrate (500 μ M). Cells were harvested in lysis buffer (150 mM NaCl, 20 mM Tris, 0.1% NP-40, 5 mM MgCl₂, 10% glycerol, 300 nM TSA, 10 mM nicotinamide, 1 \times complete protease inhibitors; pH 8). Immunoprecipitation was performed using antibodies against glucocorticoid receptor (GR) and ERR α (Abcam) with rotation at 4°C for 1 h with Dynabeads[®] Protein G (Thermo Fisher Scientific). Cell lysate was added, the system was rotated at 4°C for 2 h, and elution was performed. Immunoblotting was performed using anti-GR, -ERR α , and -acetyl lysine antibodies (Abcam).

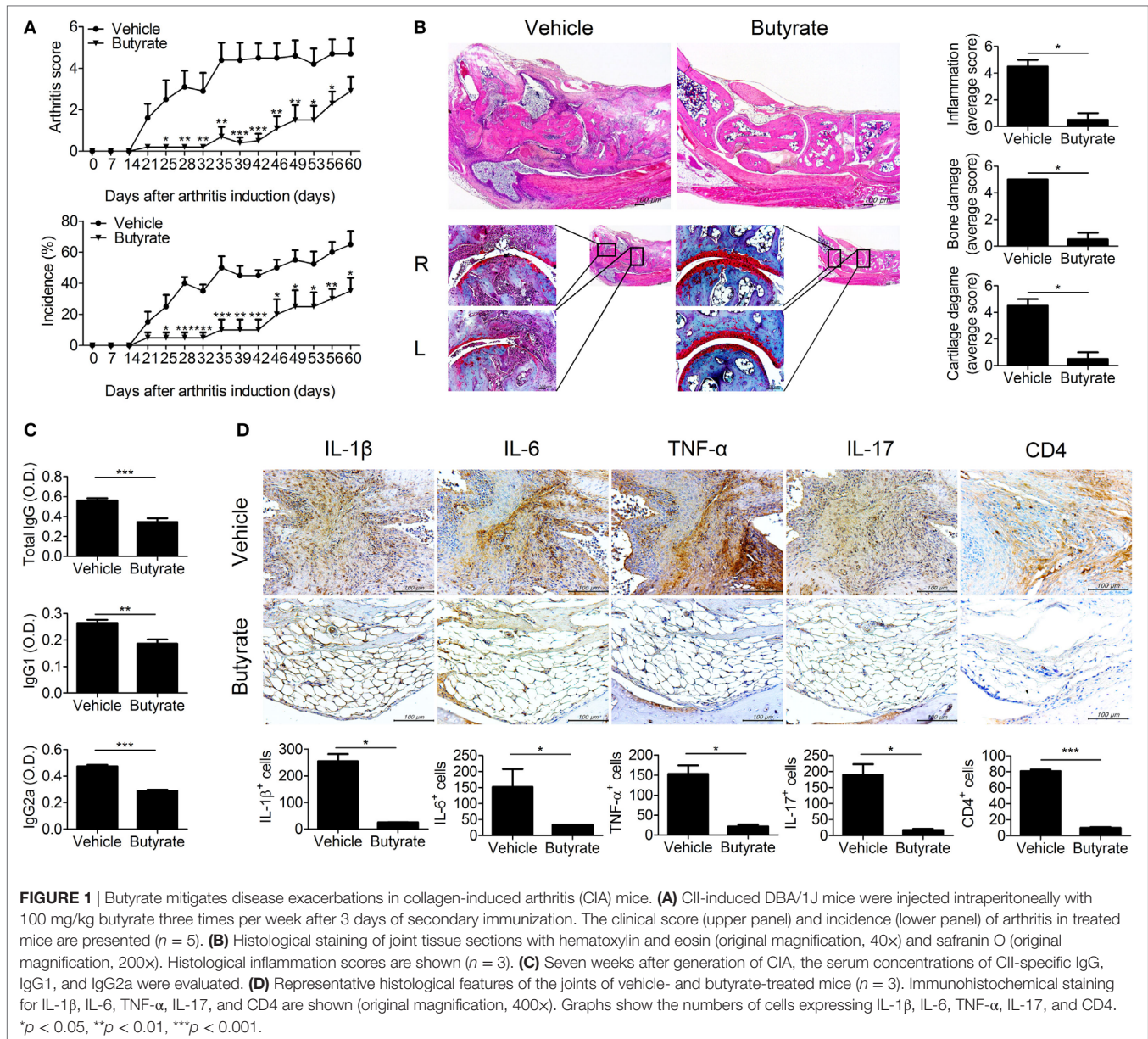
Statistical Analysis

Experiments were independently replicated at least twice, and representative and/or summary data are shown. Variation in the distribution of results was examined using the Shapiro–Wilk test. Data are presented as means \pm SD. Comparisons of the numerical data obtained from two groups were performed by Student's *t*-test or the Mann–Whitney *U*-test. Differences in the mean values of various groups were subjected to analysis of variance and a *post hoc* test. *p*-Values less than 0.05 (two-tailed) were considered indicative of statistical significance. All statistical analyses were performed using SAS software (version 9.2; SAS Institute, Cary, NC, USA).

RESULTS

Butyrate Reduced the Severity of Arthritis in the CIA Mouse Model

We administered butyrate to CIA mice. The arthritis scores and the incidence of arthritis were dramatically reduced by butyrate compared to vehicle treatment (**Figure 1A**). Histological evaluation of joint tissues showed that bone and cartilage damage was almost completely reversed by treatment with butyrate. The inflammation, bone damage, and cartilage damage scores were markedly reduced in the joints of butyrate-treated mice compared to vehicle-treated mice (**Figure 1B**). Serum CII-specific IgG, IgG1, and IgG2a levels were also reduced by administration of butyrate (**Figure 1C**). These data suggest that butyrate ameliorates CIA. Moreover, the expression levels of IL-17, IL-1 β , IL-6, and TNF- α in joint tissues were markedly reduced by treatment with butyrate compared to vehicle (**Figure 1D**). The joint tissues from vehicle-treated mice exhibited infiltrated lymphocytes, but



butyrate treatment restored the level of fat in the joint. CD4⁺ T cell infiltration in synovial tissues was markedly reduced by butyrate treatment. Finally, butyrate markedly reduced the expression of inflammatory cytokines by various cell types, demonstrating its suppressive effect on CIA.

Butyrate Inhibits Osteoclastogenesis

Bone destruction, which is mediated by osteoclasts, is directly related to the prognosis of RA patients. Therefore, we assessed the effect of butyrate on osteoclastogenesis. Inhibition of HDAC suppresses osteoclastogenesis by enhancing IFN- β production (18). *In vivo* treatment with butyrate markedly reduced expression of TRAP, a marker of osteoclasts, in synovial tissue from CIA mice (Figure 2A). Mouse bone-marrow cells were stimulated with M-CSF and RANKL to induce osteoclastogenesis with or without

butyrate; butyrate inhibited the formation of osteoclasts *in vitro* (Figure 2B). The mRNA levels of the osteoclastogenic markers including carbonic anhydrase II, TRAP, integrin β 3, DC-stamp, MMP-9, and calcitonin receptor were significantly decreased by butyrate treatment in a dose-dependent manner (Figure 2C). In particular, 1 mM butyrate treatment suppressed the expression of these markers almost completely.

Butyrate Controls Glucocorticoid Receptors by Inhibiting HDAC2, Resulting in Induction of SLPI and Attenuation of Osteoclastogenesis

Histone deacetylases inhibitors suppress osteoclastogenesis and reduce bone destruction (18, 19) and butyrate inhibits HDACs.

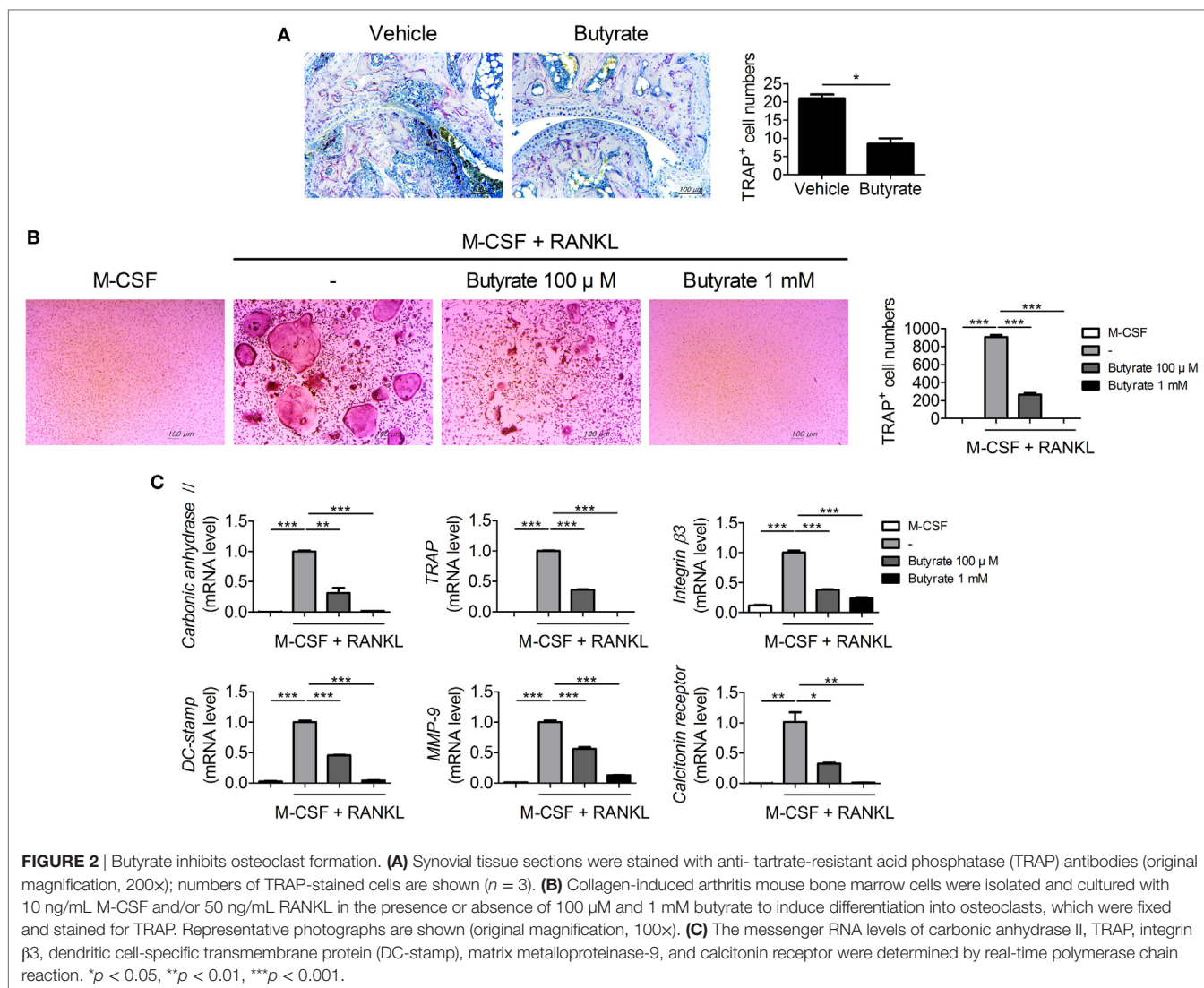


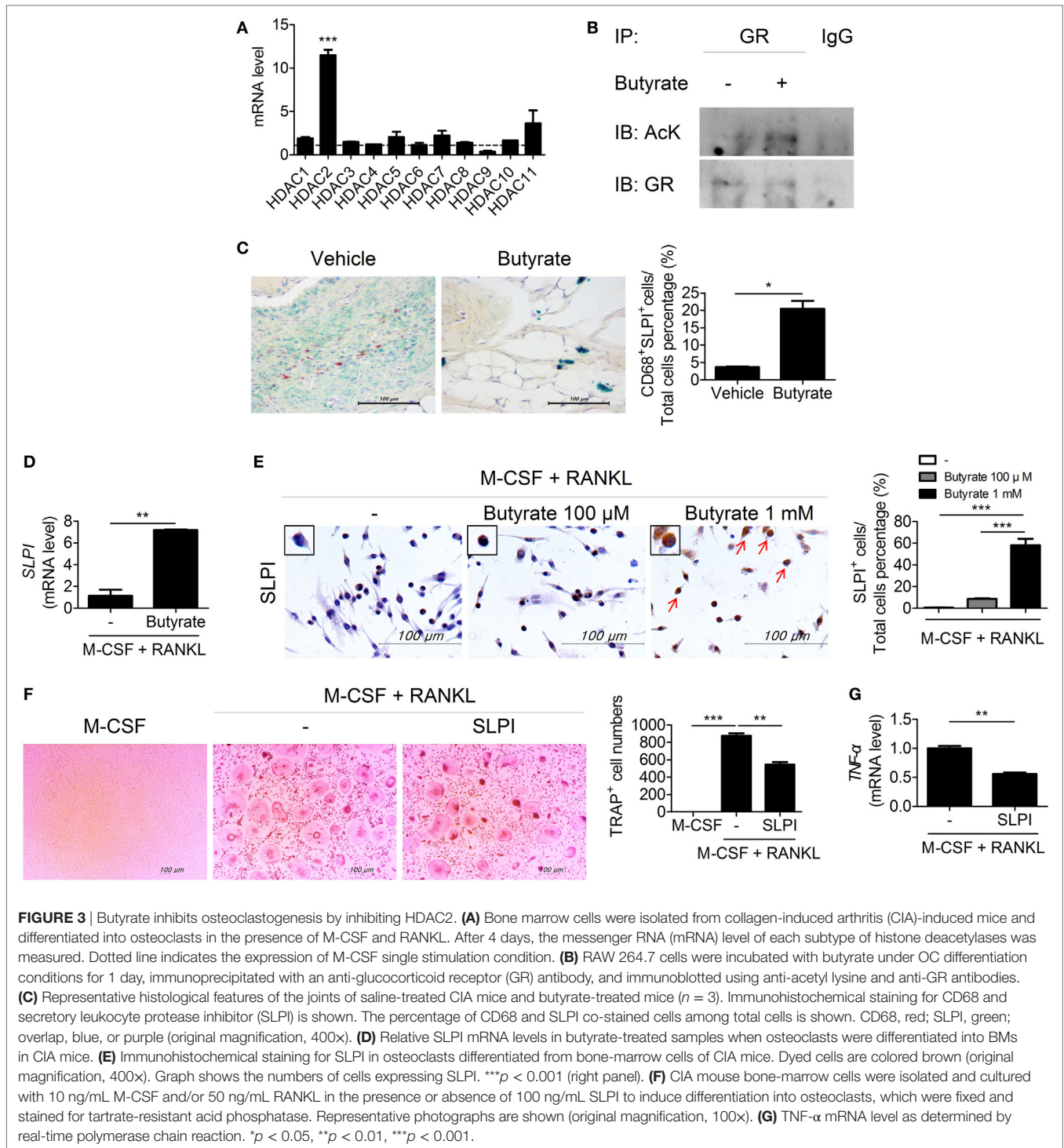
FIGURE 2 | Butyrate inhibits osteoclast formation. **(A)** Synovial tissue sections were stained with anti-tartrate-resistant acid phosphatase (TRAP) antibodies (original magnification, 200 \times); numbers of TRAP-stained cells are shown ($n = 3$). **(B)** Collagen-induced arthritis mouse bone marrow cells were isolated and cultured with 10 ng/mL M-CSF and/or 50 ng/mL RANKL in the presence or absence of 100 μ M and 1 mM butyrate to induce differentiation into osteoclasts, which were fixed and stained for TRAP. Representative photographs are shown (original magnification, 100 \times). **(C)** The messenger RNA levels of carbonic anhydrase II, TRAP, integrin β 3, dendritic cell-specific transmembrane protein (DC-stamp), matrix metalloproteinase-9, and calcitonin receptor were determined by real-time polymerase chain reaction. * $p < 0.05$, ** $p < 0.01$, *** $p < 0.001$.

We thus investigated the mRNA level of each HDAC subtype in osteoclastogenesis-induced bone-marrow cells from CIA mice. The mRNA level of *HDCA2* was increased during osteoclastogenesis (Figure 3A). Deacetylation of GR by HDAC2 results in repression of GR-mediated gene expression (20). Interestingly, acetylation-dependent GR increases the transcription of SLPI, which suppresses inflammation and joint damage in arthritis by downregulating TNF- α (21). Thus, we evaluated the effect of butyrate on the expression of SLPI *via* GR. Acetylation of GR in RAW 264.7 mouse macrophages cultured under osteoclast differentiation conditions was increased by butyrate treatment (Figure 3B). In the joint tissues of CIA-induced mice, the percentage of cells co-staining for CD68 and SLPI was significantly higher in the butyrate-treated group compared to the vehicle group (Figure 3C). *In vitro* treatment with butyrate increased the SLPI mRNA (Figure 3D) and protein (Figure 3E) levels in osteoclasts differentiated from BMMs of CIA mice, and the addition of recombinant SLPI inhibited osteoclastogenesis (Figure 3F) and decreased the TNF- α mRNA level (Figure 3G). TNF- α directly induces osteoclastogenesis (22, 23); therefore, the

butyrate-mediated increase in SLPI expression and decrease in TNF- α expression could lead to inhibition of osteoclastogenesis. Butyrate suppresses osteoclastogenesis by inhibiting HDAC2, which results in upregulation of the activity of GR and its substrate SLPI.

Butyrate Controls the T_H17/T_{reg} Balance

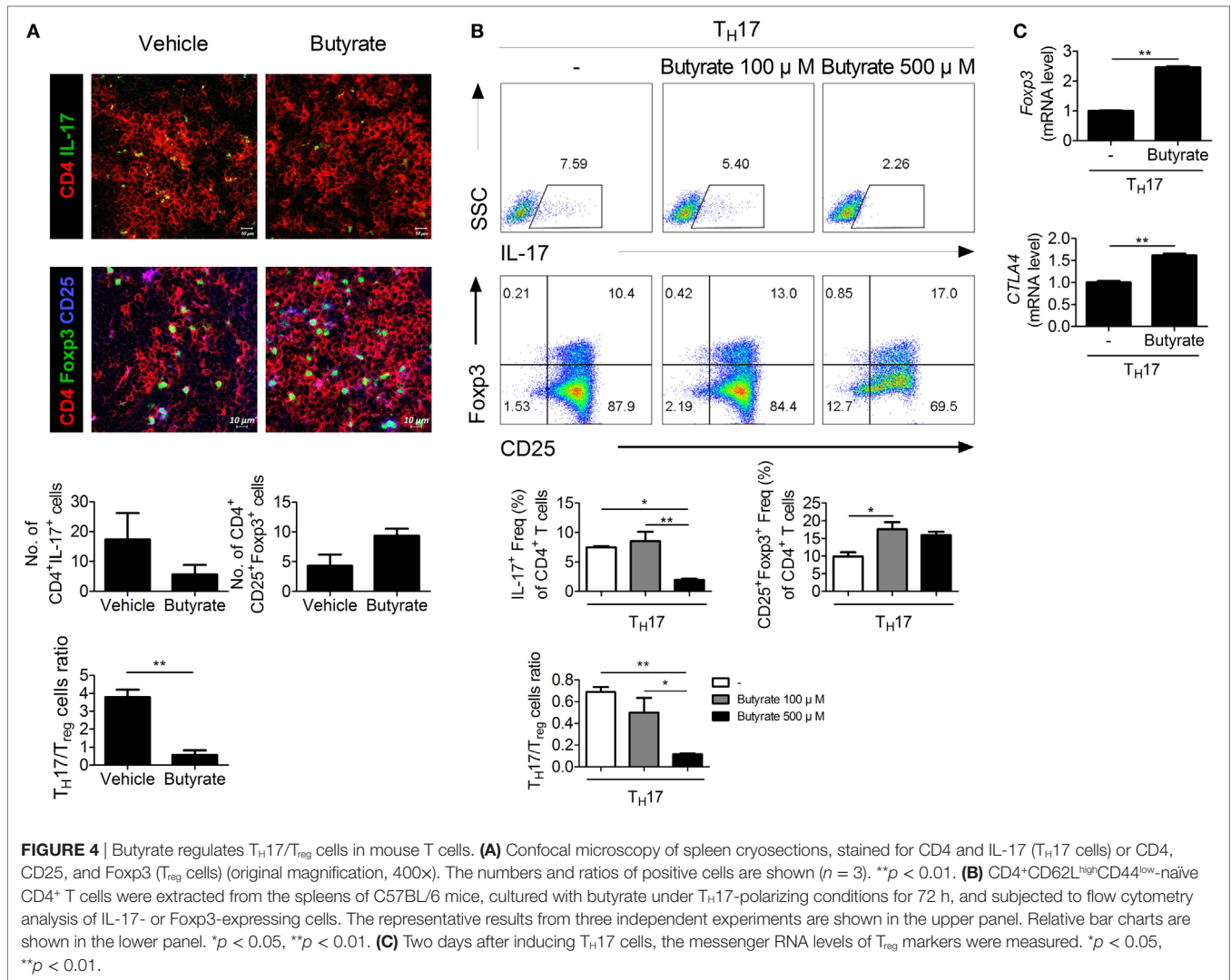
The imbalance between T_H17 and T_{reg} cells is important in RA (24–26). To assess the effect of *in vivo* treatment with butyrate on the population of T_H17 or T_{reg} cells, these cells were identified in the spleens of butyrate- or vehicle-treated CIA mice using confocal microscopy (Figure 4A). The number of IL-17-expressing CD4⁺ T cells, which are considered T_H17 cells, was significantly reduced by butyrate treatment, but the number of Treg (CD4⁺CD25⁺Foxp3⁺) cells was increased (Figure 4A). As a result, the T_H17/Treg ratio was decreased. The expression of IL-17 and Foxp3 by naive CD4⁺ T cells cultured under T_H17 differentiation conditions was reduced and increased, respectively, by *in vitro* treatment with butyrate (Figure 4B). Butyric acid did not show any cellular toxicity (Figure S2 in Supplementary Material). The T_H17/T_{reg} ratio was decreased by butyrate treatment



in a dose-dependent manner (Figure 4B). The increased number of T_{reg} cells was confirmed by the increased mRNA levels of *CTLA4* and *Foxp3* (Figure 4C). Interestingly, the level of Tyr705- or Ser727-phosphorylated STAT3, another T_{H17}/T_{reg} controller, was not changed (Figure S1 in Supplementary Material). Therefore, butyrate regulates the T-cell subtype balance irrespective of STAT3 phosphorylation; thus, it may have potential as a therapeutic agent for RA.

Butyrate Inhibits HDAC8 During T_{H17} Development, Induces CPTI, and Suppresses NR1D1 by Transactivating Estrogen-Related Receptor Alpha

To elucidate the mechanism by which butyrate affects T_{H17} cells, we next attempted to identify a T_{H17} cell-specific HDAC subtype.

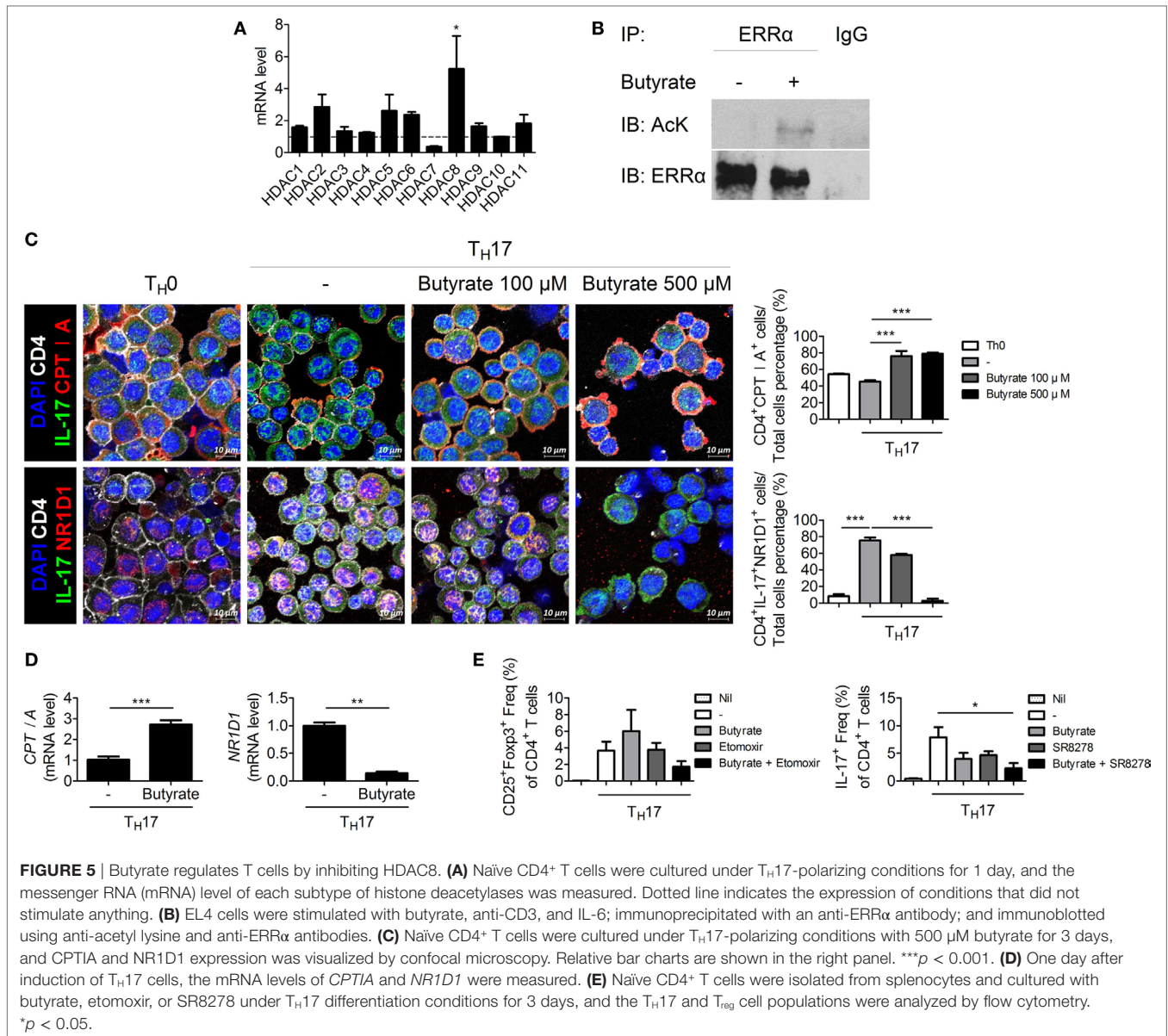


HDAC8 was highly expressed during T_H17 cell differentiation (Figure 5A). HDAC8 deacetylates estrogen-related receptor alpha ($ERR\alpha$) and enhances its transcriptional activity (27). $ERR\alpha$ is induced upon T-cell activation and controls the growth and proliferation of effector T cells (28). Butyrate treatment increased the acetylated $ERR\alpha$ level in EL4 mouse lymphocytes cultured under T_H17 differentiation conditions (Figure 5B). The decreased transcriptional activity of $ERR\alpha$ leads to an increase in the expression of carnitine palmitoyltransferase I (CPTI) (28) and a decrease in that of nuclear receptor subfamily 1, group D, member 1 (NR1D1, also known as Rev-ErbA alpha) (29). Treatment of $CD4^+$ T cells with etomoxir, a specific inhibitor of CPTI, reduces the T_{reg} population (30). Naïve NR1D1^{-/-} $CD4^+$ T cells have a decreased ability to differentiate into T_H17 cells compared to WT T-cells (31). Likewise, CPTI and NR1D1 play an important role in T_{reg} and T_H17 cells, respectively. We focused on CPTIA (also known as CPTI-L, liver isoform), which is expressed in all cells except skeletal muscle cells and brown adipose cells (32, 33). After butyrate treatment, confocal microscopy revealed that the expression of CPTIA was increased and that of NR1D1 was decreased

in T_H17 cells differentiated from naïve $CD4^+$ T cells (Figure 5C). The CPTIA and NR1D1 mRNA levels were also increased and decreased, respectively (Figure 5D). Next, naïve $CD4^+$ T cells were cultured under T_H17 differentiation conditions and treated with butyrate in the presence of etomoxir and SR8278 [inhibitors of CPTI and NR1D1, respectively (34)]. The number of T_{reg} and T_H17 cells was increased and decreased by butyrate, respectively, and these effects were enhanced in the presence of the two inhibitors (Figure 5E). Therefore, butyrate regulates the T_H17/T_{reg} cell balance by inhibiting HDAC8 through its effects on $ERR\alpha$.

Therapeutic Effect of Butyrate Is Mediated by IL-10

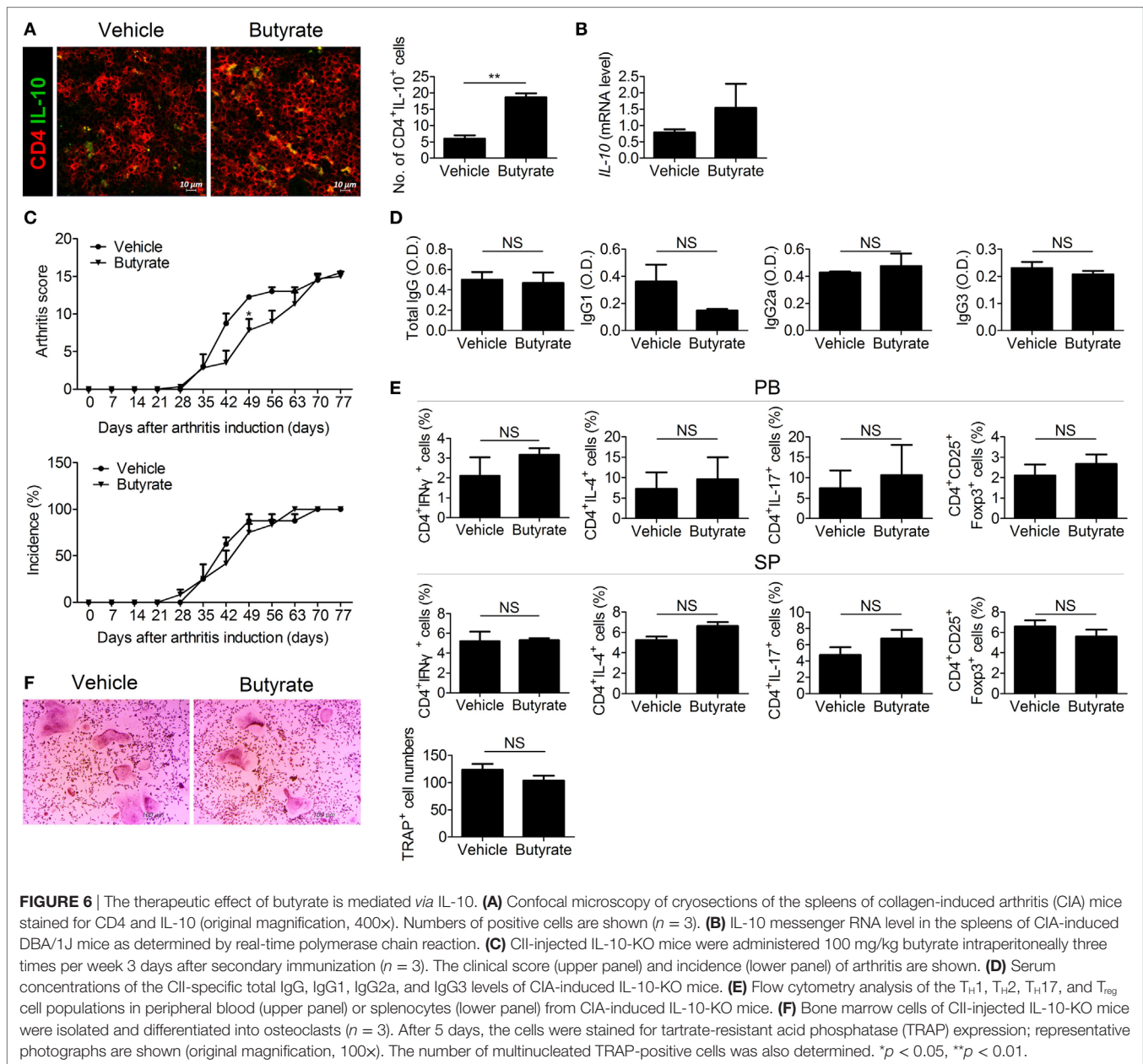
Butyrate exerts an anti-inflammatory effect by downregulating IL-12 and upregulating IL-10 (12). Some butyrate-producing *Clostridium* species are involved in T_{reg} development. IL-10-producing T_{reg} cells increase in number in mice colonized by a mixture of *Clostridiales* (35). Therefore, we assessed the role of IL-10 in the therapeutic effect of butyrate. The number of



IL-10-expressing cells (Figure 6A) and the IL-10 mRNA level (Figure 6B) were increased in the spleens of CIA mice treated with butyrate. However, butyrate treatment did not exert a significant therapeutic effect in CIA-induced IL-10-KO mice (Figure 6C). Butyrate also had little effect on the serum levels of CII-specific IgGs (Figure 6D). In the absence of IL-10, butyrate did not significantly alter the effector CD4⁺ T-cell subtype populations in the peripheral blood or spleen (Figure 6E). IL-10 inhibits bone destruction by reducing NFATc1 expression (36, 37). Therefore, we also investigated the effect of butyrate on osteoclastogenesis using BMMs from IL-10-KO mice; in the absence of IL-10, butyrate did not suppress osteoclastogenesis and did not exert a significant effect on the number of TRAP-positive MNCs (Figure 6F). Taken together, our data demonstrate that the therapeutic activity of butyrate in CIA mice is dependent on IL-10.

Effect of Butyrate on Human T_H17/T_{reg} Balance and Osteoclastogenesis

We investigated the effect of butyrate on the human T_H17/T_{reg} balance and osteoclastogenesis *in vitro*. Normal human CD4⁺ T cells were isolated and cultured under T_H17 cell-polarizing conditions with or without butyrate, and the T-cell subtype populations were analyzed by flow cytometry. The numbers of T_H17 and T_{reg} cells were dose-dependently reduced and increased, respectively, by butyrate. Also, the T_H17/T_{reg} ratio was decreased by butyrate in a dose-dependent manner, suggesting the regulation of the T_H17/T_{reg} balance by butyrate (Figure 7A). In agreement with the results using mouse cells, treatment of human PBMCs with butyrate inhibited M-CSF and RANKL-induced osteoclastogenesis (Figure 7B). Therefore, butyrate shows potential for the treatment of RA.

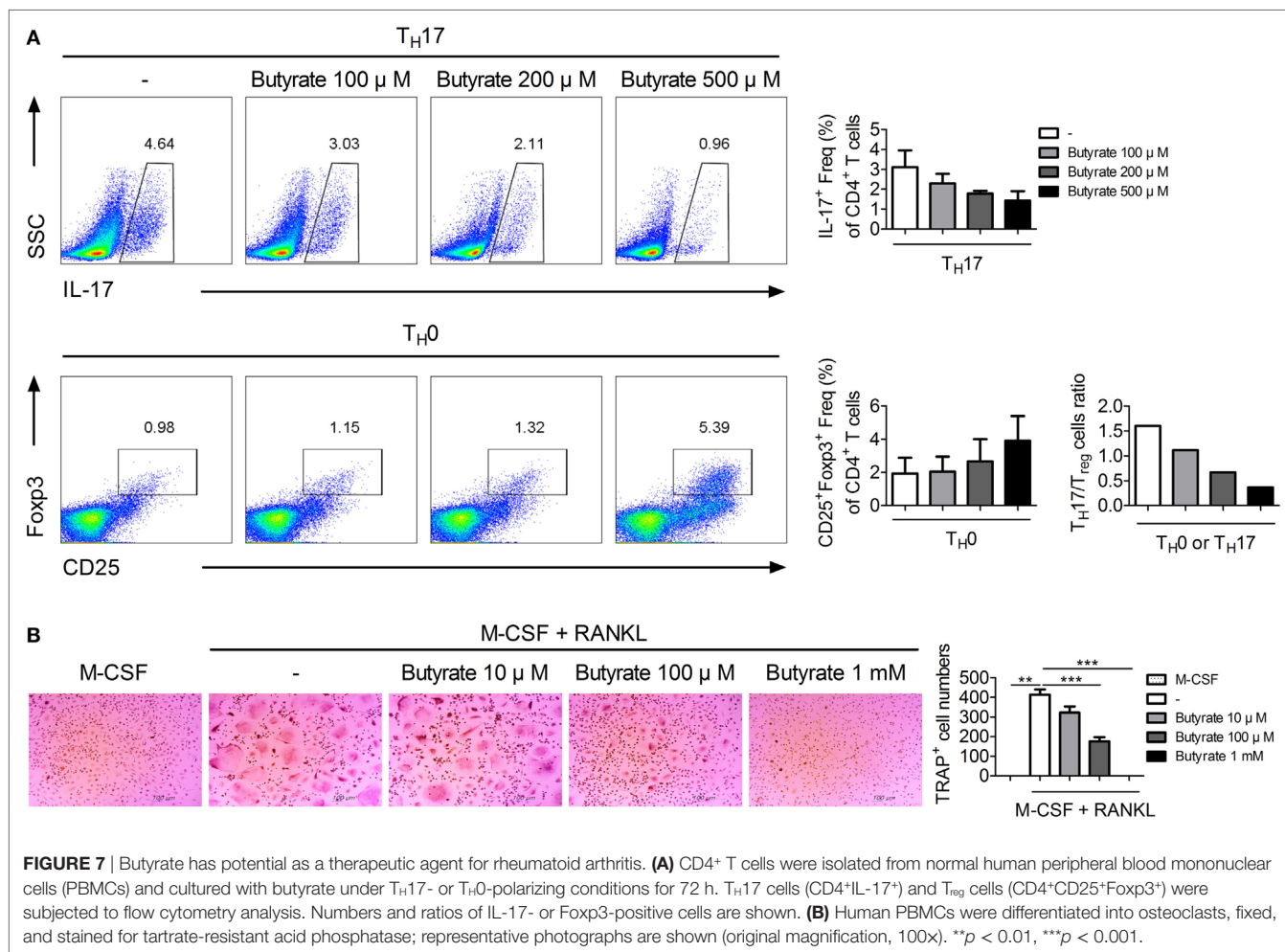


DISCUSSION

Disturbed gene expression caused by epigenetic modification can directly or indirectly lead to the development of disease. Acetylation and deacetylation are epigenetic modifications that regulate gene transcription and protein functions and are mediated by histone acetyltransferases and HDAC. For this reason, inhibitors of HDAC are used clinically to treat various conditions (38, 39). Epigenetic modification, including acetylation, of cellular proteins is involved in the pathogenesis of RA (40); this operates by modulating the activity of signaling pathways or the transcription of key factors, such as T-bet, Gata3, ROR γ t, and Foxp3, which influence the fate of effector T cells. In other words, the orchestration of gene expression or protein modification in

effector T cells may be associated with autoimmune diseases. Like butyrate, the pan-HDAC inhibitors SAHA and TSA exert therapeutic effects in RA (41, 42), but their targets and mechanisms are unclear.

Abnormal osteoclast differentiation is a major cause of RA. The gut microbiota influences bone metabolism through various pathways (5). T_H17 cells are involved in the development of various autoimmune diseases, including RA, and maintaining the T_H17 and T_{reg} balance is a challenge in the treatment of autoimmune diseases (43, 44). Microbiota is now considered important factor in T-cell homeostasis and is implicated in inflammatory diseases (45). Butyrate ameliorates autoimmune diseases (e.g., experimental allergic encephalomyelitis, GvHD, and ulcerative colitis) and is the subject of clinical trials (13, 46–49).



Also, in animal models, butyrate inhibits inflammation induced by butyrate-producing Clostridia, such as *F. prausnitzii* and *Butyricoccus pullicaecorum* (50, 51). However, few studies have focused on the therapeutic effect of butyrate on RA. Here, we report that butyrate exerts a therapeutic effect in an animal model of RA and recovers the T_H17/T_{reg} imbalance and osteoclastogenesis. We also assessed the mechanism(s) underlying the anti-arthritis effect of butyrate.

In CIA mice, parameters related to joint destruction, inflammation, expression of proinflammatory cytokines, and osteoclast formation were recovered by butyrate treatment (Figures 1 and 2). Moreover, we elucidated the mechanism by which butyrate modulates osteoclastogenesis and effector T-cell differentiation, which are critical in the pathogenesis of RA.

Deletion of HDAC7 and HDAC3 decreases and increases, respectively, bone destruction (52, 53). HDAC9 inhibits osteoclastogenesis *via* a different pathway than HDAC3 (54). In this study, the expression of HDAC2 was increased during osteoclastogenesis (Figure 3). HDAC2 upregulates RANKL-induced osteoclastogenesis by activating Akt, which results in FoxO1 depletion and interference of HDAC2 abrogates TRAP-positive osteoclasts *in vitro* (55). Butyrate reduced TRAP expression and proposed pathway of HDAC2-related GR-SLPI axis affecting

osteoclastogenesis. Akt negatively regulates GR expression (56); thus, inhibition of the HDAC2-related pathway may interrupt the Akt-related pathway, resulting in osteoclast differentiation. Butyrate inhibited expression of HDAC2, which inhibits transcription of GR by deacetylation, leading to upregulation of SLPI expression. SLPI protects epithelial tissue from serine proteases (57–60), and reportedly reduces inflammation and joint damage in arthritis (21). This is the first report that inhibition of HDAC2 by butyrate upregulates SLPI expression in osteoclasts.

HDAC8 is expressed specifically during T_H17 development, and inhibition of HDAC8 induces apoptosis of T-cell lymphoma cells (61). Its target ERR α is related to immune responses involving effector T cells and macrophages. ERR α controls the development of effector T cells, and suppression of its expression in T cells ameliorates experimental autoimmune encephalomyelitis (28). ERR α negatively regulates toll-like receptor-induced inflammation, and ERR α -deficient mice are susceptible to endotoxin-induced septic shock (62). Therefore, reduced deacetylation of ERR α by butyrate may ameliorate autoimmune diseases. In our study, butyrate decreased and increased the numbers of T_H17 and T_{reg} cells, respectively, and exerted a therapeutic effect in a mouse model of arthritis by modulating the T_H17/T_{reg} balance *in vivo* and *in vitro* (Figure 4). Regulation of the T_H17/T_{reg} balance by

and M-JP, DK and J-GR performed the animal experiments. EK, K-AJ, and J-WC conducted immunohistochemistry experiments. DK and J-EK wrote the manuscript along with input from SL, EK, Y-MM, M-LC, and S-KK. DK, J-EK, EK, M-JP, S-HP, M-LC, and S-KK discussed and developed the study concept. All authors critically reviewed and approved the final form of the manuscript.

FUNDING

This research was supported by the Bio & Medical Technology Development Program of the National Research Foundation (NRF) & funded by the Korean government (MSIT) (No.NRF-2017M3A9F3041045) and (No. NRF-2017R1A2B3007688).

REFERENCES

- Harris ED Jr. Rheumatoid arthritis. Pathophysiology and implications for therapy. *N Engl J Med* (1990) 322(18):1277–89. doi:10.1056/NEJM199005033221805
- Horta-Baas G, Romero-Figueroa MDS, Montiel-Jarquín AJ, Pizano-Zarate ML, Garcia-Mena J, Ramirez-Duran N. Intestinal dysbiosis and rheumatoid arthritis: a link between gut microbiota and the pathogenesis of rheumatoid arthritis. *J Immunol Res* (2017) 2017:4835189. doi:10.1155/2017/4835189
- Maeda Y, Takeda K. Role of gut microbiota in rheumatoid arthritis. *J Clin Med* (2017) 6(6):60. doi:10.3390/jcm6060060
- Laukens D, Brinkman BM, Raes J, De Vos M, Vandenabeele P. Heterogeneity of the gut microbiome in mice: guidelines for optimizing experimental design. *FEMS Microbiol Rev* (2016) 40(1):117–32. doi:10.1093/femsre/fuv036
- Xu X, Jia X, Mo L, Liu C, Zheng L, Yuan Q, et al. Intestinal microbiota: a potential target for the treatment of postmenopausal osteoporosis. *Bone Res* (2017) 5:17046. doi:10.1038/boneres.2017.46
- Ivanov II, Frutos Rde L, Manel N, Yoshinaga K, Rifkin DB, Sartor RB, et al. Specific microbiota direct the differentiation of IL-17-producing T-helper cells in the mucosa of the small intestine. *Cell Host Microbe* (2008) 4(4):337–49. doi:10.1016/j.chom.2008.09.009
- Ivanov II, Atarashi K, Manel N, Brodie EL, Shima T, Karaoz U, et al. Induction of intestinal Th17 cells by segmented filamentous bacteria. *Cell* (2009) 139(3):485–98. doi:10.1016/j.cell.2009.09.033
- Atarashi K, Tanoue T, Ando M, Kamada N, Nagano Y, Narushima S, et al. Th17 cell induction by adhesion of microbes to intestinal epithelial cells. *Cell* (2015) 163(2):367–80. doi:10.1016/j.cell.2015.08.058
- Park J, Kim M, Kang SG, Jannasch AH, Cooper B, Patterson J, et al. Short-chain fatty acids induce both effector and regulatory T cells by suppression of histone deacetylases and regulation of the mTOR–S6K pathway. *Mucosal Immunol* (2015) 8(1):80–93. doi:10.1038/mi.2014.44
- Correa-Oliveira R, Fachi JL, Vieira A, Sato FT, Vinolo MA. Regulation of immune cell function by short-chain fatty acids. *Clin Transl Immunology* (2016) 5(4):e73. doi:10.1038/cti.2016.17
- Furusawa Y, Obata Y, Fukuda S, Endo TA, Nakato G, Takahashi D, et al. Commensal microbe-derived butyrate induces the differentiation of colonic regulatory T cells. *Nature* (2013) 504(7480):446–50. doi:10.1038/nature12721
- Saemann MD, Bohmig GA, Osterreicher CH, Burtscher H, Parolini O, Diakos C, et al. Anti-inflammatory effects of sodium butyrate on human monocytes: potent inhibition of IL-12 and up-regulation of IL-10 production. *FASEB J* (2000) 14(15):2380–2. doi:10.1096/fj.00-0359fj
- Mathewson ND, Jenq R, Mathew AV, Koenigsnecht M, Hanash A, Toubai T, et al. Gut microbiome-derived metabolites modulate intestinal epithelial cell damage and mitigate graft-versus-host disease. *Nat Immunol* (2016) 17(5):505–13. doi:10.1038/ni.3400
- Ji J, Shu D, Zheng M, Wang J, Luo C, Wang Y, et al. Microbial metabolite butyrate facilitates M2 macrophage polarization and function. *Sci Rep* (2016) 6:24838. doi:10.1038/srep24838
- Lin HV, Frassetto A, Kowalik EJ Jr, Nawrocki AR, Lu MM, Kosinski JR, et al. Butyrate and propionate protect against diet-induced obesity and regulate gut

SUPPLEMENTARY MATERIAL

The Supplementary Material for this article can be found online at <https://www.frontiersin.org/articles/10.3389/fimmu.2018.01525/full#supplementary-material>.

FIGURE S1 | Regulation of T cells by butyrate is independent of phosphorylation of STAT3. (A) pSTAT3 Y705, pSTAT3 S727, and STAT3 expression in splenocytes from C57BL/6 mice was analyzed by western blotting; a representative figure is shown. (B) pSTAT3 Y705, pSTAT3 S727, and STAT3 expression in CD4⁺ T cells from C57BL/6 mice was analyzed by western blotting; a representative figure is shown.

FIGURE S2 | The viability of naïve T cells from normal mice treated with butyrate. The cell viability was measured using CCK assay after treatment with indicated concentrations of butyrate.

- hormones via free fatty acid receptor 3-independent mechanisms. *PLoS One* (2012) 7(4):e35240. doi:10.1371/journal.pone.0035240
- Wang X, He G, Peng Y, Zhong W, Wang Y, Zhang B. Sodium butyrate alleviates adipocyte inflammation by inhibiting NLRP3 pathway. *Sci Rep* (2015) 5:12676. doi:10.1038/srep12676
- Stoll ML, Kumar R, Morrow CD, Lefkowitz EJ, Cui X, Genin A, et al. Altered microbiota associated with abnormal humoral immune responses to commensal organisms in enthesitis-related arthritis. *Arthritis Res Ther* (2014) 16(6):486. doi:10.1186/s13075-014-0486-0
- Nakamura T, Kukita T, Shobuie T, Nagata K, Wu Z, Ogawa K, et al. Inhibition of histone deacetylase suppresses osteoclastogenesis and bone destruction by inducing IFN- β production. *J Immunol* (2005) 175(9):5809–16. doi:10.4049/jimmunol.175.9.5809
- Williams PJ, Nishu K, Rahman MM. HDAC inhibitor trichostatin A suppresses osteoclastogenesis by upregulating the expression of C/EBP- β and MKP-1. *Ann N Y Acad Sci* (2011) 1240:18–25. doi:10.1111/j.1749-6632.2011.06286.x
- Ito K, Yamamura S, Essilfie-Quaye S, Cosio B, Ito M, Barnes PJ, et al. Histone deacetylase 2-mediated deacetylation of the glucocorticoid receptor enables NF- κ B suppression. *J Exp Med* (2006) 203(1):7–13. doi:10.1084/jem.20050466
- Song X, Zeng L, Jin W, Thompson J, Mizel DE, Lei K, et al. Secretory leukocyte protease inhibitor suppresses the inflammation and joint damage of bacterial cell wall-induced arthritis. *J Exp Med* (1999) 190(4):535–42. doi:10.1084/jem.190.4.535
- Azuma Y, Kaji K, Katogi R, Takeshita S, Kudo A. Tumor necrosis factor- α induces differentiation of and bone resorption by osteoclasts. *J Biol Chem* (2000) 275(7):4858–64. doi:10.1074/jbc.275.7.4858
- Kobayashi K, Takahashi N, Jimi E, Udagawa N, Takami M, Kotake S, et al. Tumor necrosis factor α stimulates osteoclast differentiation by a mechanism independent of the ODF/RANKL-RANK interaction. *J Exp Med* (2000) 191(2):275–86. doi:10.1084/jem.191.2.275
- Kimura A, Kishimoto T. IL-6: regulator of Treg/Th17 balance. *Eur J Immunol* (2010) 40(7):1830–5. doi:10.1002/eji.201040391
- Tabarkiewicz J, Pogoda K, Karczmarczyk A, Pozarowski P, Giannopoulos K. The role of IL-17 and Th17 lymphocytes in autoimmune diseases. *Arch Immunol Ther Exp (Warsz)* (2015) 63(6):435–49. doi:10.1007/s00005-015-0344-z
- Tada Y, Ono N, Suematsu R, Tashiro S, Sadanaga Y, Tokuda Y, et al. The balance between Foxp3 and Ror- γ expression in peripheral blood is altered by tocilizumab and abatacept in patients with rheumatoid arthritis. *BMC Musculoskelet Disord* (2016) 17:290. doi:10.1186/s12891-016-1137-1
- Wilson BJ, Tremblay AM, Deblois G, Sylvain-Drolet G, Giguere V. An acetylation switch modulates the transcriptional activity of estrogen-related receptor α . *Mol Endocrinol* (2010) 24(7):1349–58. doi:10.1210/me.2009-0441
- Michalek RD, Gerriets VA, Nichols AG, Inoue M, Kazmin D, Chang CY, et al. Estrogen-related receptor- α is a metabolic regulator of effector T-cell activation and differentiation. *Proc Natl Acad Sci U S A* (2011) 108(45):18348–53. doi:10.1073/pnas.1108856108
- Deblois G, Hall JA, Perry MC, Laganieri J, Ghahremani M, Park M, et al. Genome-wide identification of direct target genes implicates estrogen-related

- receptor alpha as a determinant of breast cancer heterogeneity. *Cancer Res* (2009) 69(15):6149–57. doi:10.1158/0008-5472.CAN-09-1251
30. Michalek RD, Gerriets VA, Jacobs SR, Macintyre AN, MacIver NJ, Mason EF, et al. Cutting edge: distinct glycolytic and lipid oxidative metabolic programs are essential for effector and regulatory CD4+ T cell subsets. *J Immunol* (2011) 186(6):3299–303. doi:10.4049/jimmunol.1003613
 31. Yu X, Rollins D, Ruhn KA, Stubblefield JJ, Green CB, Kashiwada M, et al. TH17 cell differentiation is regulated by the circadian clock. *Science* (2013) 342(6159):727–30. doi:10.1126/science.1243884
 32. Brown NF, Hill JK, Esser V, Kirkland JL, Corkey BE, Foster DW, et al. Mouse white adipocytes and 3T3-L1 cells display an anomalous pattern of carnitine palmitoyltransferase (CPT) I isoform expression during differentiation. Inter-tissue and inter-species expression of CPT I and CPT II enzymes. *Biochem J* (1997) 327(Pt 1):225–31. doi:10.1042/bj3270225
 33. Lee J, Ellis JM, Wolfgang MJ. Adipose fatty acid oxidation is required for thermogenesis and potentiates oxidative stress-induced inflammation. *Cell Rep* (2015) 10(2):266–79. doi:10.1016/j.celrep.2014.12.023
 34. Kojetin D, Wang YJ, Kamenecka TM, Burris TP. Identification of SR8278, a synthetic antagonist of the nuclear heme receptor REV-ERB. *ACS Chem Biol* (2011) 6(2):131–4. doi:10.1021/cb1002575
 35. Atarashi K, Tanoue T, Shima T, Imaoka A, Kuwahara T, Momose Y, et al. Induction of colonic regulatory T cells by indigenous *Clostridium* species. *Science* (2011) 331(6015):337–41. doi:10.1126/science.1198469
 36. Zhang Q, Chen B, Yan F, Guo J, Zhu X, Ma S, et al. Interleukin-10 inhibits bone resorption: a potential therapeutic strategy in periodontitis and other bone loss diseases. *Biomed Res Int* (2014) 2014:284836. doi:10.1155/2014/284836
 37. Evans KE, Fox SW. Interleukin-10 inhibits osteoclastogenesis by reducing NFATc1 expression and preventing its translocation to the nucleus. *BMC Cell Biol* (2007) 8:4. doi:10.1186/1471-2121-8-4
 38. Hull EE, Montgomery MR, Leyva KJ. HDAC inhibitors as epigenetic regulators of the immune system: impacts on cancer therapy and inflammatory diseases. *Biomed Res Int* (2016) 2016:8797206. doi:10.1155/2016/8797206
 39. Falkenberg KJ, Johnstone RW. Histone deacetylases and their inhibitors in cancer, neurological diseases and immune disorders. *Nat Rev Drug Discov* (2014) 13(9):673–91. doi:10.1038/nrd4360
 40. Cuddapah S, Barski A, Zhao K. Epigenomics of T cell activation, differentiation, and memory. *Curr Opin Immunol* (2010) 22(3):341–7. doi:10.1016/j.coi.2010.02.007
 41. Choo QY, Ho PC, Tanaka Y, Lin HS. Histone deacetylase inhibitors MS-275 and SAHA induced growth arrest and suppressed lipopolysaccharide-stimulated NF-kappaB p65 nuclear accumulation in human rheumatoid arthritis synovial fibroblastic E11 cells. *Rheumatology (Oxford)* (2010) 49(8):1447–60. doi:10.1093/rheumatology/keq108
 42. Jungel A, Baresova V, Ospelt C, Simmen BR, Michel BA, Gay RE, et al. Trichostatin A sensitises rheumatoid arthritis synovial fibroblasts for TRAIL-induced apoptosis. *Ann Rheum Dis* (2006) 65(7):910–2. doi:10.1136/ard.2005.044065
 43. Eisenstein EM, Williams CB. The T(reg)/Th17 cell balance: a new paradigm for autoimmunity. *Pediatr Res* (2009) 65(5 Pt 2):26R–31R. doi:10.1203/PDR.0b013e31819e76c7
 44. Noack M, Miossec P. Th17 and regulatory T cell balance in autoimmune and inflammatory diseases. *Autoimmun Rev* (2014) 13(6):668–77. doi:10.1016/j.autrev.2013.12.004
 45. Lee N, Kim WU. Microbiota in T-cell homeostasis and inflammatory diseases. *Exp Mol Med* (2017) 49(5):e340. doi:10.1038/emm.2017.36
 46. Dasgupta S, Zhou Y, Jana M, Banik NL, Pahan K. Sodium phenylacetate inhibits adoptive transfer of experimental allergic encephalomyelitis in SJL/J mice at multiple steps. *J Immunol* (2003) 170(7):3874–82. doi:10.4049/jimmunol.170.7.3874
 47. Scheppach W, Sommer H, Kirchner T, Paganelli GM, Bartram P, Christl S, et al. Effect of butyrate enemas on the colonic mucosa in distal ulcerative colitis. *Gastroenterology* (1992) 103(1):51–6. doi:10.1016/0016-5085(92)91094-K
 48. Vieira EL, Leonel AJ, Sad AP, Beltrao NR, Costa TF, Ferreira TM, et al. Oral administration of sodium butyrate attenuates inflammation and mucosal lesions in experimental acute ulcerative colitis. *J Nutr Biochem* (2012) 23(5):430–6. doi:10.1016/j.jnutbio.2011.01.007
 49. Zhang M, Zhou Q, Dorfman RG, Huang X, Fan T, Zhang H, et al. Butyrate inhibits interleukin-17 and generates Tregs to ameliorate colorectal colitis in rats. *BMC Gastroenterol* (2016) 16(1):84. doi:10.1186/s12876-016-0500-x
 50. Eeckhaut V, Machiels K, Perrier C, Romero C, Maes S, Flahou B, et al. *Butyricoccus pullicaecorum* in inflammatory bowel disease. *Gut* (2013) 62(12):1745–52. doi:10.1136/gutjnl-2012-303611
 51. Sokol H, Pigneur B, Watterlot L, Lakhdari O, Bermudez-Humaran LG, Gratadoux JJ, et al. *Faecalibacterium prausnitzii* is an anti-inflammatory commensal bacterium identified by gut microbiota analysis of Crohn's disease patients. *Proc Natl Acad Sci U S A* (2008) 105(43):16731–6. doi:10.1073/pnas.0804812105
 52. Stemig M, Astelford K, Emery A, Cho JJ, Allen B, Huang TH, et al. Deletion of histone deacetylase 7 in osteoclasts decreases bone mass in mice by interactions with MITF. *PLoS One* (2015) 10(4):e0123843. doi:10.1371/journal.pone.0123843
 53. Pham L, Kaiser B, Romsa A, Schwarz T, Gopalakrishnan R, Jensen ED, et al. HDAC3 and HDAC7 have opposite effects on osteoclast differentiation. *J Biol Chem* (2011) 286(14):12056–65. doi:10.1074/jbc.M110.216853
 54. Jin Z, Wei W, Huynh H, Wan Y. HDAC9 inhibits osteoclastogenesis via mutual suppression of PPARgamma/RANKL signaling. *Mol Endocrinol* (2015) 29(5):730–8. doi:10.1210/me.2014-1365
 55. Dou C, Li N, Ding N, Liu C, Yang X, Kang F, et al. HDAC2 regulates FoxO1 during RANKL-induced osteoclastogenesis. *Am J Physiol Cell Physiol* (2016) 310(10):C780–7. doi:10.1152/ajpcell.00351.2015
 56. Piovani E, Yu J, Tosello V, Herranz D, Ambesi-Impiombato A, Da Silva AC, et al. Direct reversal of glucocorticoid resistance by AKT inhibition in acute lymphoblastic leukemia. *Cancer Cell* (2013) 24(6):766–76. doi:10.1016/j.ccr.2013.10.022
 57. McElvaney NG, Nakamura H, Birrer P, Hebert CA, Wong WL, Alphonso M, et al. Modulation of airway inflammation in cystic fibrosis. In vivo suppression of interleukin-8 levels on the respiratory epithelial surface by aerosolization of recombinant secretory leukoprotease inhibitor. *J Clin Invest* (1992) 90(4):1296–301. doi:10.1172/JCI115994
 58. Lentsch AB, Yoshidome H, Warner RL, Ward PA, Edwards Secretary MJ. Leukocyte protease inhibitor in mice regulates local and remote organ inflammatory injury induced by hepatic ischemia/reperfusion. *Gastroenterology* (1999) 117(4):953–61. doi:10.1016/S0016-5085(99)70355-0
 59. Gipson TS, Bless NM, Shanley TP, Crouch LD, Bleavins MR, Younkin EM, et al. Regulatory effects of endogenous protease inhibitors in acute lung inflammatory injury. *J Immunol* (1999) 162(6):3653–62.
 60. Zheng D, Gui B, Gray KP, Tinay I, Rafiei S, Huang Q, et al. Secretory leukocyte protease inhibitor is a survival and proliferation factor for castration-resistant prostate cancer. *Oncogene* (2016) 35(36):4807–15. doi:10.1038/onc.2016.13
 61. Balasubramanian S, Ramos J, Luo W, Sirisawad M, Verner E, Buggy JJ. A novel histone deacetylase 8 (HDAC8)-specific inhibitor PCI-34051 induces apoptosis in T-cell lymphomas. *Leukemia* (2008) 22(5):1026–34. doi:10.1038/leu.2008.9
 62. Yuk JM, Kim TS, Kim SY, Lee HM, Han J, Dufour CR, et al. Orphan nuclear receptor ERRalpha controls macrophage metabolic signaling and A20 expression to negatively regulate TLR-induced inflammation. *Immunity* (2015) 43(1):80–91. doi:10.1016/j.immuni.2015.07.003

Conflict of Interest Statement: Author K-AJ was employed by company Impact Biotech. All other authors declare no competing interests.

Copyright © 2018 Kim, Kwon, Lee, Kim, Ryu, Jung, Choi, Park, Moon, Park, Cho and Kwok. This is an open-access article distributed under the terms of the Creative Commons Attribution License (CC BY). The use, distribution or reproduction in other forums is permitted, provided the original author(s) and the copyright owner are credited and that the original publication in this journal is cited, in accordance with accepted academic practice. No use, distribution or reproduction is permitted which does not comply with these terms.